Redox Chemistry

DOI: 10.1002/anie.201208392

Syntheses and Structural Studies of Tris(*N*-phenothiazinyl)borane and Its Radical Cation**

*Shuichi Suzuki, Kohei Yoshida, Masatoshi Kozaki, and Keiji Okada**

π-Conjugated systems containing p-block elements other than carbon, nitrogen, and oxygen (such as B, Al, and P) have received growing interest in the last few decades because of their potential physicochemical properties based on the Lewis acid or base properties of these elements.[1,2] Open shell molecules incorporating these elements have also emerged under such a background,[2,3] some of which are stable and provide important structural information regarding chemical bonds with odd electrons.[2a,3f,g,4] We have focused on the B–N bond, which may be considered as a zwitterionic double bond in the neutral state (**A**), as shown in Scheme 1. According to previous crystal structure analyses of tris(amino)-

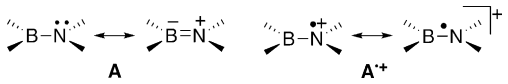

Scheme 1. Resonance structures of B–N bonds in the neutral (**A**) and oxidized (**A**$^{\bullet+}$) states.

organoboranes, the B–N bond lengths are typically in the range of 1.40–1.45 Å;[5] for example, tris(dimethylamino)borane (1.43–1.44 Å)[5a] or tris(methylphenylamino)borane (1.44–1.45 Å).[5b] However, how does the situation alter if the nitrogen center is oxidized (**A**$^{\bullet+}$)? We can consider two extreme situations: One is a bond avoiding the interaction between the vacant p orbital of boron and the cationic nitrogen p orbital; the other is that formed by a one-electron bond. To the best of our knowledge, there have been no experimental reports on tris(amino)organoborane radical cations to date. Herein, we report syntheses, structures, and properties of tris(*N*-phenothiazinyl)borane (**1**) and its radical cation (**1**$^{\bullet+}$). Comparison of the crystal structures of **1** and **1**$^{\bullet+}$ provides the first experimental insight into the electronic structure of **A**$^{\bullet+}$.

Compound **1** was prepared from phenothiazine (PTZ) as shown in Scheme 2. Lithiation of phenothiazine by *n*-butyl-

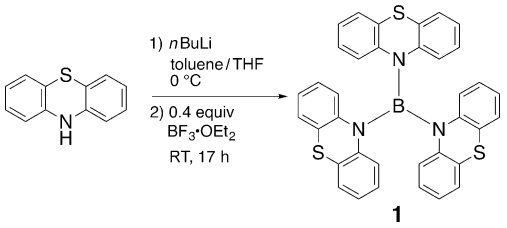

Scheme 2. Synthesis of tris(*N*-phenothiazinyl)borane (**1**).

lithium in toluene/THF was followed by treatment with boron trifluoride to give **1** in 58% yield as a colorless solid. The compound was easily handled under aerated conditions because of its stability to oxygen and moisture in both solution and solid states.

We obtained single crystals of **1** suitable for X-ray crystal structure analysis by recrystallization from a mixture of ethyl acetate and *n*-hexane.[6] The crystal structure is shown in Figure 1. All of the PTZ moieties had folded structures along

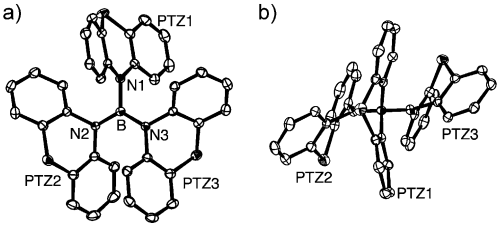

Figure 1. Crystal structure of **1**. a) Top and b) side views. Hydrogen atoms are omitted for clarity. Thermal ellipsoids set at 50%. Selected bond lengths [Å]: B–N1 = 1.488(2), B–N2 = 1.429(2), B–N3 = 1.435(2).

the N–S axis (butterfly structure).[7] The folded angle (27.1°) of PTZ1 is slightly smaller than those of PTZ2 and PTZ3 (49.3° and 50.8°, respectively). The summation of the bond angles around the nitrogen atoms, N1, N2, and N3, was almost 360° (359.9° for PTZ1, 359.7° for PTZ2, and 359.8° for PTZ3), indicating sp^2 hybridization for these nitrogen atoms. The dihedral angle between Plane N*n* (defined by B, N*n* (*n* = 1, 2, or 3), and the two sp^2 carbon atoms directly attached to N*n*) and Plane B (defined by B, N1, N2, and N3) were 86.4° for Plane N1/Plane B, 20.6° for Plane N2/Plane B, and 12.5° for Plane N3/Plane B. The small angles for Plane N2/Plane B and Plane N3/Plane B indicated the nearly parallel orientation between the vacant p orbital of the B atom and the lone-pair p orbital of the N2 and N3 atoms, whereas the larger dihedral angle for Plane N1/Plane B indicated a twisted

[*] Dr. S. Suzuki, K. Yoshida, Dr. M. Kozaki, Prof. Dr. K. Okada
Department of Chemistry, Graduate School of Science, Osaka City University, 3-3-138, Sugimoto, Sumiyoshi-ku
Osaka 558-8585 (Japan)
E-mail: okadak@sci.osaka-cu.ac.jp

[**] This work was partially supported by a Grant-in-Aid for Scientific Research from JSPS (22350066 to K.O.) and a Grant-in-Aid for Scientific Research on Innovative Areas "Emergence of Highly Elaborated π-Space and Its Function" from MEXT (23108717 to S.S.). S.S. also thanks the Asahi Glass Foundation and the Tokuyama Science Foundation for financial support.

Supporting information for this article is available on the WWW under http://dx.doi.org/10.1002/anie.201208392.

© 2013 Wiley-VCH Verlag GmbH & Co. KGaA, Weinheim

orientation for PTZ1. Accordingly, the bond length of B–N1 (1.488(2) Å) was slightly longer than those of B–N2 (1.429(2) Å) and B–N3 (1.435(2) Å).

We examined the temperature-dependent ^{1}H NMR spectra of **1** (Figure 2). Owing to PTZ, conspicuous pairs of triplet and doublet peaks were seen at 273 K, and twelve distinct

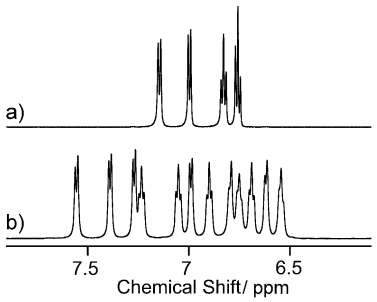

Figure 2. NMR spectra of **1** at a) 273 K and b) 173 K in [D_8]THF.

protons corresponding to the three sets of PTZ groups were clearly observed at 173 K. The twelve distinct protons at low temperature in solution are compatible with the X-ray structure (Figure 1) in a pseudo-C_2 symmetry, assuming rapid ring inversion of the PTZ1 ring. The observed spectral change is thus consistent with the conformational change from C_3 symmetry (273 K) to C_2 symmetry (173 K) by rapid proton exchange through cooperative transformation of the PTZ rings (PTZ1→PTZ2→PTZ3→PTZ1) through B–N bond rotations and ring inversions. The spectral change was analyzed using an NMR simulation program,[8] providing the rate parameters of $\Delta H^{\neq} = 39.6\ \mathrm{kJ\,mol^{-1}}$ and $\Delta S^{\neq} = -4.43\ \mathrm{J\,K^{-1}\,mol^{-1}}$ (see the Supporting Information for details).

The cyclic voltammogram of **1** showed a reversible oxidation wave E_{ox}^{1} at +0.20 V vs. Fc/Fc$^+$ and an irreversible oxidation wave E_{ox}^{2} at around +1.2 V as a peak potential (E_{ox}^{1} in Figure 3 inset, see also Supporting Information). The E_{ox}^{1} value was similar to the one-electron oxidation potential of the model compounds, 10-(4′-*tert*-butylphenyl)-10*H*-phenothiazine (**2**) and *N*-methylphenpthiazine (**3**; see the Supporting Information). To identify the oxidized species, we monitored absorption spectra using a thin-layer cell during electrochemical oxidation through the application of an

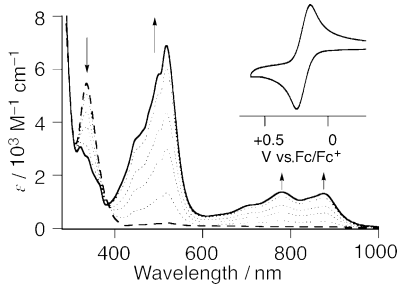

Figure 3. UV/Vis spectral changes during electrochemical oxidation of **1**: The dashed and solid lines show the spectra of **1** and **1**$^{\bullet+}$, respectively. The dotted lines show intermediate states. Inset: cyclic voltammogram of **1** in CH_2Cl_2.

external potential of +0.40 V, which is sufficiently high to oxidize **1**. The observed spectral change is shown in Figure 3. The UV/Vis spectrum of **1** before oxidation showed an absorption at $\lambda_{max} = 335$ nm and no absorption in visible region. During electrochemical oxidation, new absorption bands appeared at $\lambda_{max} = 516$, 778, and 874 nm. These spectral shapes and molar absorption coefficients were quite similar to those of **2**$^{\bullet+}$ (see the Supporting Information), which suggests quantitative formation of monoradical cation species **1**$^{\bullet+}$, in which the spin and charge are localized on only one of the PTZ rings. The absorption owing to **1**$^{\bullet+}$ was irreversibly decreased by further electrochemical oxidation over +1.2 V, which suggests that the **1**$^{2+}$ species is unstable.

We could isolate **1**$^{\bullet+}$ by chemical oxidation. An acetonitrile solution of thianthrenium tetrachlorogallate salt was added to a dichloromethane solution of **1** to give the desired **1**$^{\bullet+}$·$GaCl_4^-$ as a deep red solid. The UV/Vis spectrum of this compound was consistent with that in Figure 3 (see also Figure S7 in the Supporting Information). The electron spin resonance (ESR) spectrum recorded in dichloromethane revealed complicated splittings with $g = 2.0054$ (Figure 4), which could be reproduced by spectral simulation with the aid of calculated hyperfine coupling constants using the *Gaussian 09* program[9] on the X-ray determined structure. In the simulation, the ratio of hyperfine couplings, $|a^{10B}|/|a^{11B}|$, was assumed to be 0.335,[3b] based on the ratio of nuclear *g* factors of ^{10}B and ^{11}B.[10]

The presence of two non-equivalent hyperfine couplings of the nitrogen atoms ($|a^N| = 0.627$ mT (1N) and 0.087 mT (2N) in Figure 4) indicates the localized radical cation structure in one of the PTZ rings in **1**$^{\bullet+}$ as well as the slow intramolecular hole migration in the ESR time scale at room temperature.

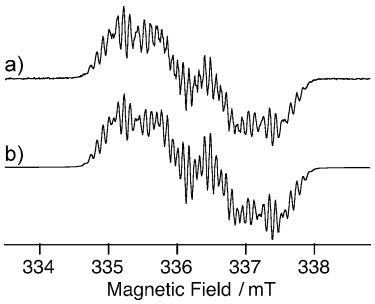

Figure 4. a) Observed ESR spectrum of **1**$^{\bullet+}$·$GaCl_4^-$ recorded in CH_2Cl_2 at room temperature. b) Simulated ESR spectrum of **1**$^{\bullet+}$·$GaCl_4^-$. Parameters for simulation: $g = 2.0054$, $\nu_0 = 9.447031$ MHz, $|a^N| = 0.6265$ mT, $|a^N|$ (×2) = 0.0873 mT, $|a^{11B}| = 0.2842$ mT, $|a^{10B}| = 0.0952$ mT,[10] $|a^H|$ (×2, respectively) = 0.2248, 0.0947, 0.0699, 0.0272 mT (for details, see Figure S9 in the Supporting Information).

Single crystals of **1**$^{\bullet+}$·$GaCl_4^-$ suitable for X-ray crystal structure analysis were obtained by recrystallization from dichloromethane/benzene.[11] The crystal structure is shown in Figure 5. The overall structure was similar to **1** and possessed a pseudo-C_2 symmetry (**1**$^{\bullet+}$: 80.7° for Plane N1/Plane B, 8.1° for Plane N2/Plane B, and 8.9° for Plane N3/Plane B). Interestingly, the structure of the PTZ radical cation and those of neutral PTZ groups could be easily distinguished in the X-ray

 © 2013 Wiley-VCH Verlag GmbH & Co. KGaA, Weinheim

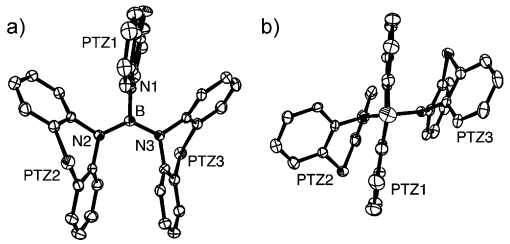

Figure 5. Crystal structure of $\mathbf{1}^{\bullet+}\cdot GaCl_4^-$. a) Top and b) side views. Hydrogen atoms and counteranion are omitted for clarity. Thermal ellipsoids set at 50 %. Selected bond lengths [Å]: B–N1 = 1.529(6), B–N2 = 1.423(5), B–N3 = 1.410(5).

structure; in contrast to the other two PTZ moieties (PTZ2, PTZ3), PTZ1 had a planar structure, which shows that the radical cation is localized on the PTZ1 ring. Importantly, the longest B–N1 bond (B–N1: 1.529(6) Å) was clearly distinguishable from the other two B–N bonds (B–N2: 1.423(5) Å, and B–N3: 1.410(5) Å).

The elongation of the B–N1 bond is explained by unfavorable electronic interactions between the vacant B p orbital and the cationic N p orbital. Because of the positively charged PTZ1 ring, the B atom in $\mathbf{1}^{\bullet+}$ became much more electron deficient than that in neutral **1**. For this reason, the B–N2 and B–N3 bond lengths in $\mathbf{1}^{\bullet+}$ became slightly shorter than those in neutral **1**. A similar effect also led to higher coplanarity in Plane N2/Plane B and Plane N3/Plane B in $\mathbf{1}^{\bullet+}$ (see above), with the cationic PTZ1 unit being nearly perpendicular to Plane B.

In summary, we have designed and synthesized tris(*N*-phenothiazinyl)borane (**1**). The radical cation $\mathbf{1}^{\bullet+}$ was prepared by chemical oxidation, and was found to be stable to air in both solution and solid states. The absorption and ESR spectra of $\mathbf{1}^{\bullet+}$ consistently showed that the spin and charge were localized to one of the PTZ rings. X-ray structure analysis clearly established elongation of the B–N bond directly bound to the PTZ radical cation, resulting from unfavorable electronic interactions between the vacant B p orbital and the cationic N p orbital. Related studies of open shell molecules involving p block elements are in progress.

Received: October 18, 2012
Published online: January 21, 2013

Keywords: boranes · main group elements · radical ions · redox chemistry

[1] For example: a) J. E. Anthony, *Chem. Rev.* **2006**, *106*, 5028–5048; b) M. Elbing, G. C. Bazan, *Angew. Chem.* **2008**, *120*, 846–850; *Angew. Chem. Int. Ed.* **2008**, *47*, 834–838; c) T. Baumgartner, R. Réau, *Chem. Rev.* **2006**, *106*, 4681–4727; d) A. Fukazawa, S. Yamaguchi, *Chem. Asian J.* **2009**, *4*, 1386–1400; e) P. G. Campbell, A. J. V. Marwitz, S.-Y. Liu, *Angew. Chem.* **2012**, *124*, 6178–6197; *Angew. Chem. Int. Ed.* **2012**, *51*, 6074–6092; f) A. Osuka, E. Tsurumaki, T. Tanaka, *Bull. Chem. Soc. Jpn.* **2011**, *84*, 679–697; g) Z. Zhou, A. Wakamiya, T. Kushida, S. Yamaguchi, *J. Am. Chem. Soc.* **2012**, *134*, 4529–4532.

[2] a) P. P. Power, *Chem. Rev.* **2003**, *103*, 789–809; b) J. Konu, T. Chivers in *Stable Radicals: Fundamentals and Applied Aspects of Odd-Electron Compounds* (Ed.: R. G. Hicks), Wiley, Chichester, **2010**, pp. 381–406.

[3] a) A. Lichtblau, W. Kaim, A. Schulz, T. Stahl, *J. Chem. Soc. Perkin Trans. 2* **1992**, 1497–1501; b) W. Kaim, N. S. Hosmane, S, Záliš, J. A. Maguire, W. N. Lipscomb, *Angew. Chem.* **2009**, *121*, 5184–5193; *Angew. Chem. Int. Ed.* **2009**, *48*, 5082–5091; c) A. Rajca, S. Rajca, S. R. Desai, *J. Chem. Soc. Chem. Commun.* **1995**, 1957–1958; d) K. Okada, T. Kawata, M. Oda, *J. Chem. Soc. Chem. Commun.* **1995**, 233–234; e) R. Suzuki, M. Oda, A. Kajiwara, M. Kamachi, M. Kozaki, Y. Morimoto, K. Okada, *Tetrahedron Lett.* **1998**, *39*, 6483–6486; f) C.-W. Chiu, F. P. Gabbaï, *Angew. Chem.* **2007**, *119*, 1753–1755; *Angew. Chem. Int. Ed.* **2007**, *46*, 1723–1725; g) C.-W. Chiu, F. P. Gabbaï, *Angew. Chem.* **2007**, *119*, 7002–7005; *Angew. Chem. Int. Ed.* **2007**, *46*, 6878–6881; h) T. K. Wood, W. E. Piers, B. A. Keay, M. Parvez, *Chem. Commun.* **2009**, 5147–5149; i) S. M. Mansell, C. J. Adams, G. Bramham, M. F. Haddow, W. Kaim, N. C. Norman, J. E. McGrady, C. A. Russell, S. J. Udeen, *Chem. Commun.* **2010**, *46*, 5070–5072; j) B. T. King, B. C. Noll, A. J. McKinley, J. Michl, *J. Am. Chem. Soc.* **1996**, *118*, 10902–10903; k) S. K. Pal, M. E. Itkis, F. S. Tham, R. W. Reed, R. T. Oakley, R. C. Haddon, *Science* **2005**, *309*, 281–284.

[4] For chemical bonds with odd electrons, see: a) L. Pauling, *J. Am. Chem. Soc.* **1931**, *53*, 3225–3237; b) H. Klusik, A. Berndt *Angew. Chem.* **1981**, *93, 903–904; Angew. Chem. Int. Ed. Engl.* **1981**, 20, 870–871; *Angew. Chem. Int. Ed. Engl.* **1981**, *20*, 870–871; c) M. Seierstad, C. R. Kinsinger, C. J. Cramer, *Angew. Chem.* **2002**, *114*, 4050–4052; *Angew. Chem. Int. Ed.* **2002**, *41*, 3894–3896; d) H. Grützmacher, F. Breher, *Angew. Chem.* **2002**, *114*, 4178–4184; *Angew. Chem. Int. Ed.* **2002**, *41*, 4006–4011; e) A. Rodriguez, R. A. Olsen, N. Ghaderi, D. Scheschkewitz, F. S. Tham, L. J. Mueller, G. Bertrand, *Angew. Chem.* **2004**, *116*, 4988–4991; *Angew. Chem. Int. Ed.* **2004**, *43*, 4880–4883.

[5] a) G. Schmid, R. Boese, D. Blaser, *Z. Naturforsch. B* **1982**, *37*, 1230–1233; b) H. Noth, S. Weber, *Z. Naturforsch. B* **1983**, *38*, 1460–1465; c) B. Wrackmeyer, B. Schwarze, W. Milius, *Inorg. Chim. Acta* **1996**, *241*, 87–93.

[6] Crystallographic data for **1**: triclinic, space group: $P\bar{1}$ (#2), a = 8.0000(2) Å, b = 10.8200(4) Å, c = 17.2700(10) Å, α = 87.290(7)°, β = 87.630(7)°, γ = 75.080(6)°, V = 1442.22(11) Å^3, Z = 2, ρ_{calc} = 1.394 g cm^{-3}, T = 150(2) K, R = 0.0424, wR = 0.0894, GOF = 1.085. CCDC 904593 contains the supplementary crystallographic data for this paper. These data can be obtained free of charge from The Cambridge Crystallographic Data Centre via www.ccdc.cam.ac.uk/data_request/cif.

[7] a) J. J. H. McDowell, *Acta Crystallogr. Sect. B* **1976**, *32*, 5–10; b) B. Moerman, M. Ouwerkerk, J. Kroon, *Acta Crystallogr. Sect. C* **1985**, *41*, 1205–1208; c) T. Okamoto, M. Kuratsu, M. Kozaki, K. Hirotsu, A. Ichimura, T. Matsushita, K. Okada, *Org. Lett.* **2004**, *6*, 3493–3496.

[8] gNMR ver. 5 obtained from Adept Scientific.

[9] *Gaussian 09*, Revision A.02, M. J. Frisch, G. W. Trucks, H. B. Schlegel, G. E. Scuseria, M. A. Robb, J. R. Cheeseman, G. Scalmani, V. Barone, B. Mennucci, G. A. Petersson, H. Nakatsuji, M. Caricato, X. Li, H. P. Hratchian, A. F. Izmaylov, J. Bloino, G. Zheng, J. L. Sonnenberg, M. Hada, M. Ehara, K. Toyota, R. Fukuda, J. Hasegawa, M. Ishida, T. Nakajima, Y. Honda, O. Kitao, H. Nakai, T. Vreven, J. A. Montgomery, Jr., J. E. Peralta, F. Ogliaro, M. Bearpark, J. J. Heyd, E. Brothers, K. N. Kudin, V. N. Staroverov, R. Kobayashi, J. Normand, K. Raghavachari, A. Rendell, J. C. Burant, S. S. Iyengar, J. Tomasi, M. Cossi, N. Rega, J. M. Millam, M. Klene, J. E. Knox, J. B. Cross, V. Bakken, C. Adamo, J. Jaramillo, R. Gomperts, R. E. Stratmann, O. Yazyev, A. J. Austin, R. Cammi, C. Pomelli, J. W. Ochterski, R. L. Martin, K. Morokuma, V. G. Zakrzewski, G. A.

 © 2013 Wiley-VCH Verlag GmbH & Co. KGaA, Weinheim

Voth, P. Salvador, J. J. Dannenberg, S. Dapprich, A. D. Daniels, Ö. Farkas, J. B. Foresman, J. V. Ortiz, J. Cioslowski, D. J. Fox, Gaussian, Inc., Wallingford CT, **2009**.

[10] J. A. Weil, J. R. Bolton, *Electron Paramagnetic Resonance*, 2nd ed., Wiley, New York, **2007**.

[11] Crystallographic data for $\mathbf{1}^{\bullet+}\cdot GaCl_4^-$: orthorhombic, space group: $P2_12_12_1$ (#19), $a = 13.353(2)$ Å, $b = 15.9154(19)$ Å, $c = 16.264(2)$ Å, $V = 3456.5(8)$ Å^3, $Z = 4$, $\rho_{calc} = 1.570\ g\,cm^{-3}$, $T = 150(1)$ K, $R = 0.0573$, $wR = 0.1539$, GOF = 0.963. CCDC 904594 contains the supplementary crystallographic data for this paper. These data can be obtained free of charge from The Cambridge Crystallographic Data Centre via www.ccdc.cam.ac.uk/data_request/cif.

 © 2013 Wiley-VCH Verlag GmbH & Co. KGaA, Weinheim